Bi-directional Task-Guided Network for Few-Shot Fine-Grained Image Classification

Zhen-Xiang Ma
Shandong University
Jinan, China
mazhenxiang0923@163.com

Zhen-Duo Chen*
Shandong University
Jinan, China
chenzd.sdu@gmail.com

Li-Jun Zhao
Shandong University
Jinan, China
lj_zhao1028@163.com

Zi-Chao Zhang
Shandong University
Jinan, China
zhangzichao1008@163.com

Tai Zheng
Shandong University
Jinan, China
zt5369623@gmail.com

Xin Luo
Shandong University
Jinan, China
luoxin.lxin@gmail.com

Xin-Shun Xu
Shandong University
Jinan, China
xuxinshun@sdu.edu.cn

Abstract

In recent years, the Few-Shot Fine-Grained Image Classification (FS-FGIC) problem has gained widespread attention. A number of effective methods have been proposed that focus on extracting discriminative information within high-level features in a single episode/task. However, this is insufficient for addressing the cross-task challenges of FS-FGIC, which is represented in two aspects. On the one hand, from the perspective of the Fine-Grained Image Classification (FGIC) task, there is a need to supplement the model with mid-level features containing rich fine-grained information. On the other hand, from the perspective of the Few-Shot Learning (FSL) task, explicit modeling of cross-task general knowledge is required. In this paper, we propose a novel Bi-directional Task-Guided Network (BTG-Net) to tackle these issues. Specifically, from the FGIC task perspective, we design the Semantic-Guided Noise Filtering (SGNF) module to filter noise on mid-level features rich in detailed information. Further, from the FSL task perspective, the General Knowledge Prompt Modeling (GKPM) module is proposed to retain the cross-task general knowledge by utilizing the prompting mechanism, thereby enhancing the model's generalization performance on novel classes. We have conducted extensive experiments on five fine-grained benchmark datasets, and the results demonstrate that BTG-Net outperforms state-of-the-art methods comprehensively.

CCS Concepts

• **Computing methodologies** → **Visual content-based indexing and retrieval**; **Matching**.

Keywords

Few-Shot Learning, Fine-Grained Image Analysis, Prompting Mechanism

ACM Reference Format:
Zhen-Xiang Ma, Zhen-Duo Chen, Li-Jun Zhao, Zi-Chao Zhang, Tai Zheng, Xin Luo, and Xin-Shun Xu. 2024. Bi-directional Task-Guided Network for Few-Shot Fine-Grained Image Classification. In *Proceedings of the 32nd ACM International Conference on Multimedia (MM '24), October 28-November 1, 2024, Melbourne, VIC, Australia.* ACM, New York, NY, USA, 10 pages. https://doi.org/10.1145/3664647.3680593

1 Introduction

Benefiting from the rapid advancement of deep learning [10, 14], significant progress has been achieved in the computer vision task of image classification [2, 47]. These models rely on large-scale, label-rich training samples, however, the annotation process for large-scale image datasets is extremely time-consuming and cost-consuming. In contrast, humans can effortlessly learn new concepts from one or a few samples. To mitigate the model's excessive dependence on data volume, researchers are focusing on Few-Shot Learning (FSL) [21, 29, 38].

FSL aims to use extremely limited labeled support samples based on transferable knowledge from base classes, enabling models to perform well on unlabeled query samples from novel classes. A number of successful FSL methods, based on meta-learning and metric learning, have been proposed. Inspired by this, researchers have extended FSL to more challenging fine-grained datasets, introducing the novel task of Few-Shot Fine-Grained Image Classification (FS-FGIC) [44, 54].

However, as a cross-task between Fine-Grained Image Classification (FGIC) and FSL, existing methods for FS-FGIC still have shortcomings that need further improvement, this is evident in two

[*] Corresponding author.

MM '24, October 28-November 1, 2024, Melbourne, VIC, Australia

ACM ISBN 979-8-4007-0686-8/24/10
https://doi.org/10.1145/3664647.3680593

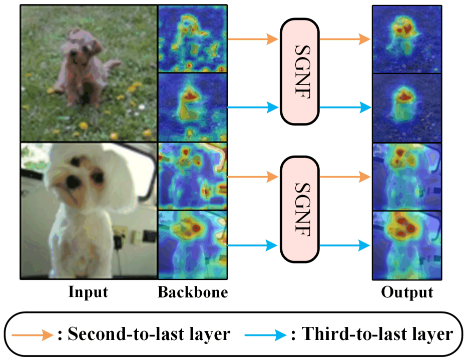

Figure 1: Visualization results of feature maps extracted by the Conv-4 Backbone and Semantic-Guided Noise Filtering (SGNF) module on the Stanford-Dogs dataset.

aspects. On the one hand, as a FGIC task [11], effective fine-grained feature extraction constitutes the foundation for models to achieve good performance. However, constrained by the issue of overfitting under the FSL setting, most existing methods [40, 46] primarily rely on the last layer features of the backbone for classification, lacking sufficient utilization of the network's feature learning capabilities. Specifically, the high-level features outputted by the last layer of the network often contain rich global semantic information, but this unavoidably results in the loss of local detailed information. Solely relying on high-level semantic features for classification is often insufficient to distinguish fine-grained images with subtle inter-class differences, thus impacting the performance of the method. Therefore, addressing the FS-FGIC task requires adequate assistance from local detailed features. Experience shows that mid-level features often contain more fine-grained information, but at the same time, they also include a significant amount of background and other trivial noise as shown in Figure 1. Directly using them will exacerbate overfitting issues under the FSL setting. On the other hand, as a FSL task, the essence of the model training process lies in learning the commonalities between different tasks (i.e., episodes) and based on this foundation, focusing on the unique characteristics of each task. The high degree of similarity between different classes in fine-grained data dictates the presence of abundant shared knowledge across various tasks, and the differences between tasks are mainly reflected in the details. Existing methods primarily confine their learning to within a single task, lacking explicit modeling of cross-task general knowledge. Clearly, under the FSL setting, especially for fine-grained datasets, general knowledge facilitates transfer learning between tasks. If the model only focuses on intra-task feature extraction, it will cause the model to overfit on the trainable base classes, preventing effective learning of task-transferable knowledge for generalization to unseen novel classes, thus affecting the performance of FS-FGIC.

To address the cross-task challenge of FS-FGIC, we propose a novel Bi-directional Task-Guided Network (BTG-Net), which contains two modules to solve the feature requirements of FS-FGIC from the perspective of two tasks respectively. From the perspective of the FGIC task, it is essential to introduce rich local detail features to assist classification, while reducing the overfitting issue as much as possible. Specifically, instead of simply concatenating high-level and mid-level features, we propose the Semantic-Guided Noise Filtering (SGNF) module to generate filters for mid-level features through high-level features with powerful target object localization capability. These filters are then employed to re-weight and adjust the mid-level features, effectively eliminating background and other trivial noises as shown in Figure 1. This process provides the model with improved fine-grained information to assist in classification. From the perspective of the FSL task, it is necessary to learn cross-task general knowledge. We design the General Knowledge Prompt Modeling (GKPM) module, which utilizes high-level features to learn cross-task general knowledge, as these semantically rich high-level features often represent general attributes of categories. Inspired by the prompting mechanism in computer vision [18], a learnable Task-General Prompt is designed to learn shared general knowledge across all tasks. By introducing cross-task general knowledge and using the self-attention mechanism of Transformer [9], the query features are further optimized to reduce the distance between query features and prototypes of the same class while distancing them from prototypes of different classes, with limited support samples. This process enables the model to maintain robust generalization capabilities on the novel classes.

In general, BTG-Net is dedicated to meeting the feature needs of both fine-grained task and few-shot learning task, and thereby achieving state-of-the-art results on five fine-grained benchmarks. Our contributions can be summarized as follows:

- We propose a novel BTG-Net that addresses the feature requirements of the FS-FGIC from the perspectives of both FGIC and FSL tasks.
- From the perspective of the FGIC task, we propose the SGNF module, which effectively filters out noise such as background in mid-level features with the assistance of semantic guidance of high-level features. This process introduces rich fine-grained information to assist FS-FGIC, while minimizing overfitting problem associated with the addition of features as much as possible.
- From the perspective of the FSL task, we propose the GKPM module. We design the Task-General Prompt to retain the cross-task general knowledge, enabling the model to exhibit strong generalization capabilities on novel tasks and classes.
- We conducted extensive experiments on five few-shot fine-grained benchmark datasets, and the results indicate that the proposed method outperforms the current state-of-the-art methods comprehensively.

2 Related Work

2.1 Few-Shot Learning

FSL aims to recognize novel classes with only a limited number of support samples provided for each class. Previous research commonly utilizes a meta-learning framework, where a model is trained on a series of few-shot training tasks/episodes randomly sampled from the base dataset to rapidly adapt to unseen testing tasks. Specifically, meta-learning based methods [22, 30] try to discover a suitable gradient-based optimization strategy to quickly adapt to novel tasks with few gradient updates. MAML [12] aims to learn a way to initialize parameters so that the model can easily adapt to new tasks.

Data-augmentation based methods [3, 13, 35] seek to train a generator from base classes and leverage it to generate novel samples. Metric-learning based methods [33, 34, 38] focus on learning a fixed embedding function to map input images into a low-dimensional embedding space. FRN [43] uses support sample features to reconstruct query sample features for better similarity measurement.

However, traditional FSL methods, which usually pay less attention to feature learning, may not always perform well on fine-grained datasets with subtle inter-class differences. Therefore, FS-FGIC has attracted increasing attention in recent years.

2.2 Few-Shot Fine-Grained Image Classification

Expanding general FSL methods directly to fine-grained datasets does not yield satisfactory performance, therefore, Wei et al. [41] first define the FS-FGIC task and use bilinear features to train a classifier with piecewise mapping. BSNet [26] utilizes two metric functions for the joint optimization of the model. PaCL [40] employs contrastive learning to extract more discriminative features from various object regions. TDM [23] generates task-specific channel weights to localize the discriminative regions for each class. BiFRN [44] introduces a bi-reconstruction mechanism to simultaneously accommodate for inter-class and intra-class variations.

The existing method AGPF [36] attempts to aggregate multi-scale information from different layers, but it neglects that introducing mid-level features with background noise exacerbates the overfitting issue under the FSL setting. BSFA [49] proposes a two-stage background suppression and foreground alignment framework to capture subtle differences and align support and query samples. This is an operation within high-level features, neglecting the rich detailed information in mid-level features. Additionally, BFSA directly crops the background of high-level features, not simply eliminating non-generalizable background noise. In contrast, we use high-level features to filter out background noise in mid-level features, thereby providing fine-grained information to assist classification in the FS-FGIC task. Furthermore, all the mentioned methods are confined to feature learning within a single task, overlooking the necessity for exploring commonalities across FSL tasks. In contrast, our proposed method explicitly models cross-task general knowledge using the prompting mechanism, enhancing the model’s generalization capability on novel classes.

2.3 Prompting Mechanism

Inspired by prompting mechanism in the field of natural language processing [1], VPT [18] is the first to apply prompting mechanism to computer visual tasks. Existing prompt-based methods [52, 53] typically require freezing large-scale pre-trained models, designing learnable prompts for parameter-efficient fine-tuning to adapt to downstream tasks. In contrast, our proposed BTG-Net does not require pre-trained models nor parameter freezing; the entire model is trained end-to-end.

3 Method

3.1 Problem Definition

Under the standard FSL settings, the dataset $D = \{(x_i, y_i), y_i \in Y\}$ is divided into the training dataset $D_{base} = \{(x_i, y_i), y_i \in Y_{base}\}$, the validation dataset $D_{val} = \{(x_i, y_i), y_i \in Y_{val}\}$, and the test dataset $D_{novel} = \{(x_i, y_i), y_i \in Y_{novel}\}$, where x_i is the original sample, y_i is the i-th class label, and $Y_{base} \cap Y_{val} \cap Y_{novel} = \emptyset$. We adopt the episodic training mechanism. Specifically, during the training phase, each episode represents an N-way K-shot classification problem. N classes are randomly selected from D_{base}, each class having K labeled images in the support set and U unlabeled images in the query set. During the testing phase, the model is evaluated on the test dataset D_{novel}. Without loss of generality, the following discussion assumes consideration within an episode/task.

3.2 Overall Framework

To address the cross-task problem of FS-FGIC from the perspectives of both FGIC and FSL tasks, we propose the novel BTG-Net, and the overall framework is shown in Figure 2.

The BTG-Net consists of four components: The first component is the backbone network, which is used to extract deep features from the support and query samples. The second component is the SGNF Module, which takes the high-level features (output from the last layer of the backbone network) and mid-level features (from the second-to-last and third-to-last layers) as inputs. It utilizes the high-level features to perform noise filtering on the mid-level features. The third component is the GKPM module, which takes high-level features as input and utilizes the prompting mechanism to model task-general knowledge, so as to adjust query features and enhance the generalization ability of the model. The last component is the Similarity module, responsible for computing the cosine similarity between the query features and prototypes at each layer. The weighted sum of the three similarities is employed for the classification of the query samples.

3.3 Semantic-Guided Noise Filtering

Through the analysis from the perspective of the FGIC task in the introduction section, globally semantic-rich high-level features (i.e., the output of the network’s last layer) cannot effectively handle fine-grained images with subtle differences between categories. Simply concatenating mid-level features will introduce trivial noise such as background, exacerbating the overfitting issue under the FSL setting. Therefore, we designed the Semantic-Guided Noise Filtering (SGNF) module, as illustrated in Figure 2, to achieve a filtering effect of high-level features on mid-level features.

Specifically, given a sample $\mathbf{X}$, we obtain features through the backbone network f as follows,

$$\mathbf{F}_l, \mathbf{F}_s, \mathbf{F}_t = f(\mathbf{X}), \tag{1}$$

where $\mathbf{F}_l \in \mathbb{R}^{C^l \times H^l \times W^l}$, $\mathbf{F}_s \in \mathbb{R}^{C^s \times H^s \times W^s}$ and $\mathbf{F}_t \in \mathbb{R}^{C^t \times H^t \times W^t}$ represent the feature maps obtained from the last layer, second-to-last layer, and third-to-last layer, respectively.

Due to the rich global semantic information of the high-level feature $\mathbf{F}_l$, which can effectively locate the global information of the target, we use the $\mathbf{F}_l$ to generate filters for mid-level features $\mathbf{F}_s$ and $\mathbf{F}_t$. Considering the varying sizes of feature maps at different layers, we use Bilinear interpolation $B(\cdot)$ to map the size of the feature map of $\mathbf{F}_l$ to match that of $\mathbf{F}_s$ and $\mathbf{F}_t$. It is important to note that the use of bilinear interpolation does not alter the number of channels in the feature maps, thereby avoiding any loss of information. The

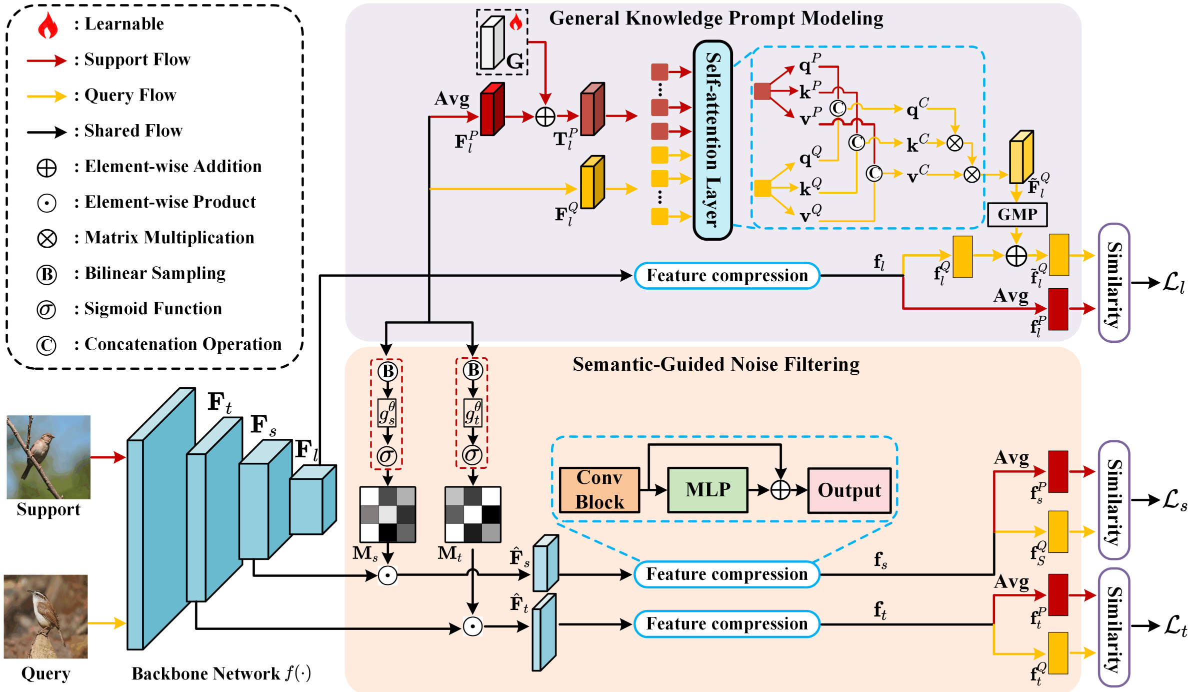

Figure 2: Overview of the Bi-directional Task-Guided Network (BTG-Net), consisting of the Backbone Network, the Semantic-Guided Noise Filtering (SGNF) module, the General Knowledge Prompt Modeling (GKPM) module, and the Similarity module.

filters can be formulated as

$$\mathbf{M}_s = \sigma(g_s^\theta(B(\mathbf{F}_l))) \in \mathbb{R}^{1\times H^s\times W^s}, \tag{2}$$

$$\mathbf{M}_t = \sigma(g_t^\theta(B(\mathbf{F}_l))) \in \mathbb{R}^{1\times H^t\times W^t}, \tag{3}$$

where g_s^θ and g_t^θ are sub-networks that include two convolutional layers each, and σ is the sigmoid activation function.

Based on $\mathbf{M}_s$ and $\mathbf{M}_t$, we can reweight and adjust the mid-level features to eliminate trivial noise such as background, which can be formulated as

$$\hat{\mathbf{F}}_s = \mathbf{F}_s \odot \mathbf{M}_s \in \mathbb{R}^{C^s\times H^s\times W^s}, \tag{4}$$

$$\hat{\mathbf{F}}_t = \mathbf{F}_t \odot \mathbf{M}_t \in \mathbb{R}^{C^t\times H^t\times W^t}, \tag{5}$$

where $\odot$ denotes element-wise product operation with the broadcasting mechanism. Next, we design the feature compression block to compress the feature spaces of $\hat{\mathbf{F}}_s$ and $\hat{\mathbf{F}}_t$, mitigating potential overfitting issues. Features $\mathbf{f}_s \in \mathbb{R}^{C^s}$ and $\mathbf{f}_t \in \mathbb{R}^{C^t}$ can be obtained as follows,

$$\mathbf{f}_s = \alpha(Conv_s(\hat{\mathbf{F}}_s)) + (1-\alpha)(MLP_s(Conv_s(\hat{\mathbf{F}}_s))), \tag{6}$$

$$\mathbf{f}_t = \alpha(Conv_t(\hat{\mathbf{F}}_t)) + (1-\alpha)(MLP_t(Conv_t(\hat{\mathbf{F}}_t))), \tag{7}$$

where $Conv_s(\cdot)$ and $Conv_t(\cdot)$ each represents convolution block with global max pooling, $MLP_s(\cdot)$ and $MLP_t(\cdot)$ each represents fully connected block, and α is a balancing hyper-parameter. Finally, query features $(\mathbf{f}_s^Q, \mathbf{f}_t^Q)$ and support features $(\mathbf{f}_s^S, \mathbf{f}_t^S)$ can be separated from $\mathbf{f}_s$ and $\mathbf{f}_t$, respectively. Following the ProtoNet [33], we generate prototypes $(\mathbf{f}_s^P, \mathbf{f}_t^P)$ for each class. The computation for the prototype for the i-th class is as follows,

$$\mathbf{f}_{s,i}^P = \frac{1}{K}\sum_{j=1}^{K}\mathbf{f}_{i,j,s}^S, \tag{8}$$

$$\mathbf{f}_{t,i}^P = \frac{1}{K}\sum_{j=1}^{K}\mathbf{f}_{i,j,t}^S. \tag{9}$$

In this module, we extensively explored the network's feature extraction capabilities. By filtering and eliminating noise from mid-level features, we provide rich local details to assist in classification for the FS-FGIC task. This procedure also alleviates overfitting issues under the FSL setting.

3.4 General Knowledge Prompt Modeling

After addressing the demand for fine-grained features from the FGIC task perspective, we further analyzed the FSL task. If the model is confined to feature learning within a single task, it can not explicitly learn transferable knowledge, resulting in overfitting on the trainable base classes and poor generalization performance on novel classes. In light of this, we designed the General Knowledge Prompt Modeling (GKPM) module as illustrated in Figure 2, employing the prompting mechanism to explicitly model cross-task general knowledge, and then introducing it into query features to ensure the model possesses robust generalization capabilities on novel classes.

Table 1: The splits of datasets, C_{train}, C_{val}, C_{test} represent the number of classes for training, validation, and test, respectively. C_{total} indicates the original number of classes.

Dataset	C_{train}	C_{val}	C_{test}	C_{total}
CUB-200-2011	100	50	50	200
Stanford-Dogs	70	20	30	120
Stanford-Cars	130	17	49	196
meta-iNat	908	-	227	1135
tiered meta-iNat	781	-	354	1135

Specifically, to express clarity, we use $\mathbf{F}_l^S \in \mathbb{R}^{C^l \times H^l \times W^l}$ and $\mathbf{F}_l^Q \in \mathbb{R}^{C^l \times H^l \times W^l}$ to represent the support and query features, respectively. Then we generate prototypes for each class as follows,

$$\mathbf{F}_{l,i}^P = \frac{1}{K} \sum_{j=1}^{K} \mathbf{F}_{i,j,l}^S. \tag{10}$$

Thereafter, inspired by the prompting mechanism, we design the learnable Task-General (TG) Prompt ($\mathbf{G} \in \mathbb{R}^{C^l \times H^l \times W^l}$) to retain cross-task general knowledge. It is important to note that the TG Prompt is shared across all tasks during the training, validation, and testing phases. To incorporate cross-task general knowledge into the specific task, we add $\mathbf{G}$ with each prototype to obtain the task generalization information, which is formulated as

$$\mathbf{T}_l^P = \mathbf{F}_l^P + \mathbf{G} \in \mathbb{R}^{C^l \times H^l \times W^l}, \tag{11}$$

we omit the subscript i for clarity in expression. Based on $\mathbf{T}_l^P$, we dynamically adjust the query features $\mathbf{F}_l^Q$ using the self-attention mechanism of the Transformer. Specifically, we flatten $\mathbf{F}_l^Q$ and $\mathbf{T}_l^P$ into $(H^l \times W^l)$ tokens, each token is C^l-dimensional. Then, we use weighted parameters W_{qkv} to map each token to the query vector $\mathbf{q}$, key vector $\mathbf{k}$, and value vector $\mathbf{v}$, as follows,

$$\mathbf{q}^Q, \mathbf{k}^Q, \mathbf{v}^Q = W_{qkv}^Q \mathbf{F}_l^Q \in \mathbb{R}^{H^l W^l \times C^l}, \tag{12}$$

$$\mathbf{q}^P, \mathbf{k}^P, \mathbf{v}^P = W_{qkv}^P \mathbf{T}_l^P \in \mathbb{R}^{H^l W^l \times C^l}. \tag{13}$$

Afterward, to adequately model the relationship between query features $\mathbf{F}_l^Q$ and the task generalization information $\mathbf{T}_l^P$, we concatenate vectors of the same type as follows,

$$\left\{ \begin{array}{l} \mathbf{q}^C = \left[\mathbf{q}^Q, \mathbf{q}^P\right] \\ \mathbf{k}^C = \left[\mathbf{k}^Q, \mathbf{k}^P\right] \\ \mathbf{v}^C = \left[\mathbf{v}^Q, \mathbf{v}^P\right] \end{array} \right. \in \mathbb{R}^{2H^l W^l \times C^l}, \tag{14}$$

where $[\cdot, \cdot]$ is the concatenation operation, then we use standard self-attention mechanism in Transformer to obtain the task generalization query features $\hat{\mathbf{F}}_l^Q$. This process can be represented as

$$\tilde{\mathbf{F}}_l^Q = \text{softmax}\left(\frac{\mathbf{q}^C (\mathbf{k}^C)^T}{(C^l)^{\frac{1}{4}}}\right) \mathbf{v}^C \in \mathbb{R}^{2H^l W^l \times C^l}. \tag{15}$$

To maintain task generalization query features with the same feature map size as the original query features, we slice $\tilde{\mathbf{F}}_l^Q$, retaining only the first HW vectors, and then reshape it back to the size of $C^l \times H^l \times W^l$, i.e. $\tilde{\mathbf{F}}_l^Q \in \mathbb{R}^{C^l \times H^l \times W^l}$.

Table 2: The accuracy (%) of 5-way 1-shot and 5-shot on CUB (using raw images) dataset. The best results are shown in bold.

Methods	Backbone	CUB	
		1-shot	5-shot
ProtoNet (NeurIPS-17) [33]	Conv-4	59.95	76.01
MattML (IJCAI-20) [54]	Conv-4	66.29	80.34
PoseNorm (CVPR-20) [37]	Conv-4	64.17	81.96
FEAT (CVPR-20) [48]	Conv-4	68.87	82.90
BSNet (TIP-21) [26]	Conv-4	55.81	76.34
FRN (CVPR-21) [43]	Conv-4	69.45	85.16
OLSA (MM-21) [45]	Conv-4	73.07	86.24
ATT-NET (AAAI-22) [46]	Conv-4	72.89	86.60
FRN + TDM (CVPR-22) [23]	Conv-4	71.37	86.45
AGPF (PR-22) [36]	Conv-4	74.03	86.54
PaCL (MM-22) [40]	Conv-4	74.04	88.75
BiFRN (AAAI-23) [44]	Conv-4	74.98	89.14
Ours	Conv-4	**79.19**	**89.71**
ProtoNet (NeurIPS-17) [33]	ResNet-12	72.99	86.65
Neg-Cosine (ECCV-20) [27]	ResNet-18	72.66	89.40
P-Transfer (AAAI-21) [31]	ResNet-12	73.16	88.32
DeepEMD (CVPR-20) [51]	ResNet-12	75.65	88.69
OLSA (MM-21) [45]	ResNet-12	77.77	89.87
FRN (CVPR-21) [43]	ResNet-12	83.55	92.92
ISC (TIP-22) [5]	ResNet-12	73.72	87.51
AGPF (PR-22) [36]	ResNet-12	78.73	89.77
PaCL (MM-22) [40]	ResNet-12	77.80	92.07
FRN + TDM (CVPR-22) [23]	ResNet-12	84.36	93.37
BSFA (TSCVT-23) [49]	ResNet-12	82.27	90.76
FGFL (ICCV-23) [4]	ResNet-12	80.77	92.01
Ventral (AAAI-23) [8]	ResNet-12	83.33	92.97
BiFRN (AAAI-23) [44]	ResNet-12	82.07	92.11
Ours	ResNet-12	**86.44**	**94.20**

The original feature $\mathbf{F}_l$ compresses the feature space in the same way as the previous module, as

$$\mathbf{f}_l = \alpha(Conv_l(\mathbf{F}_l)) + (1-\alpha)(MLP_l(Conv_l(\mathbf{F}_l))). \tag{16}$$

Based on $\mathbf{f}_l \in \mathbb{R}^{C^l}$, we can obtain query features $\mathbf{f}_l^Q$ and support features $\mathbf{f}_l^S$, and then acquire prototype $\mathbf{f}_l^P$ using the same approach as in Eq (8). Finally, we integrate task generalization query features $\tilde{\mathbf{F}}_l^Q$ into the query features to obtain a comprehensive representation that includes cross-task information, as follows,

$$\tilde{\mathbf{f}}_l^Q = \mathbf{f}_l^Q + \lambda GMP(\tilde{\mathbf{F}}_l^Q), \tag{17}$$

where λ is the learnable weight parameter and $GMP(\cdot)$ is Global Max Pooling.

Through the above procedure, we store cross-task general knowledge with the TG prompt and introduce it to optimize the query features, bringing the query closer to the prototype of the same class, further enhancing intra-class consistency feature learning with limited support samples. This aids in the FS-FGIC learning of well-transferable meta-knowledge, enabling the model to exhibit

Table 3: The accuracy (%) of 5-way 1-shot and 5-shot on Stanford-Dogs and Stanford-Cars datasets.

Methods	Backbone	Stanford-Dogs		Stanford-Cars	
		1-shot	5-shot	1-shot	5-shot
ProtoNet (NeurIPS-17) [33]	Conv-4	40.81 ± 0.83	61.58 ± 0.71	36.51 ± 0.74	62.14 ± 0.76
MattML (IJCAI-20) [54]	Conv-4	54.84 ± 0.53	71.34 ± 0.38	66.11 ± 0.54	82.80 ± 0.28
ATL-Net (IJCAI-20) [7]	Conv-4	54.49 ± 0.92	73.20 ± 0.69	67.95 ± 0.84	89.16 ± 0.48
BSNet (TIP-21) [26]	Conv-4	43.13 ± 0.85	62.61 ± 0.73	44.56 ± 0.83	63.72 ± 0.78
LRPABN (TMM-21) [17]	Conv-4	45.72 ± 0.75	60.94 ± 0.66	60.28 ± 0.76	73.29 ± 0.58
FRN (CVPR-21) [43]	Conv-4	49.37 ± 0.20	67.13 ± 0.17	58.90 ± 0.22	79.65 ± 0.15
TOAN (TCSVT-21) [16]	Conv-4	49.30 ± 0.77	67.16 ± 0.49	65.90 ± 0.72	84.24 ± 0.48
OLSA (MM-21) [45]	Conv-4	55.53 ± 0.45	71.68 ± 0.36	70.13 ± 0.48	84.29 ± 0.31
ATT-NET (AAAI-22) [46]	Conv-4	59.81 ± 0.50	77.19 ± 0.35	70.21 ± 0.50	85.55 ± 0.31
AGPF (PR-22) [36]	Conv-4	60.89 ± 0.98	78.14 ± 0.62	78.14 ± 0.84	87.42 ± 0.57
PaCL (MM-22) [40]	Conv-4	59.76 ± 0.70	77.50 ± 0.48	72.21 ± 0.68	88.02 ± 0.36
HelixFormer (MM-22) [50]	Conv-4	59.81 ± 0.50	73.40 ± 0.36	75.46 ± 0.37	89.68 ± 0.25
LCCRN (TCSVT-23) [25]	Conv-4	-	-	71.62 ± 0.21	86.41 ± 0.12
BiFRN (AAAI-23) [44]	Conv-4	61.39 ± 0.23	78.86 ± 0.15	76.22 ± 0.20	90.66 ± 0.11
Ours	Conv-4	**67.33 ± 0.52**	**81.08 ± 0.33**	**78.72 ± 0.46**	**90.78 ± 0.26**
BSNet (TIP-21) [26]	ResNet-12	61.95 ± 0.97	79.62 ± 0.63	71.07 ± 1.03	88.38 ± 0.62
OLSA (MM-21) [45]	ResNet-12	64.15 ± 0.49	78.28 ± 0.32	77.03 ± 0.46	88.85 ± 0.46
AGPF (PR-22) [36]	ResNet-12	72.34 ± 0.86	84.02 ± 0.57	85.34 ± 0.74	94.79 ± 0.35
HelixFormer (MM-22) [50]	ResNet-12	65.92 ± 0.49	80.65 ± 0.36	79.40 ± 0.43	92.26 ± 0.15
BSFA (TSCVT-23) [49]	ResNet-12	69.58 ± 0.50	82.59 ± 0.33	88.93 ± 0.38	95.20 ± 0.20
LCCRN (TCSVT-23) [25]	ResNet-12	-	-	87.04 ± 0.17	96.09 ± 0.07
BiFRN (AAAI-23) [44]	ResNet-12	72.54 ± 0.22	85.86 ± 0.13	88.43 ± 0.17	96.34 ± 0.07
Ours	ResNet-12	**76.06 ± 0.50**	**88.48 ± 0.29**	**90.28 ± 0.34**	**96.78 ± 0.15**

Table 4: The accuracy (%) of 5-way 1-shot and 5-shot on meta-iNat and tiered meta-iNat datasets using Conv-4 backbone.

Methods	meta-iNat		tiered meta-iNat	
	1-shot	5-shot	1-shot	5-shot
ProtoNet (NeurIPS-17) [33]	53.78	73.80	35.47	54.85
DN4 (CVPR-19) [24]	62.32	79.76	43.82	64.17
DSN (CVPR-20) [32]	58.08	77.38	36.82	60.11
CTX (NeurIPS-20) [6]	60.03	78.80	36.83	60.84
DeepEMD (CVPR-20) [51]	54.48	68.36	36.05	48.55
FRN (CVPR-21) [43]	61.98	80.04	43.95	63.45
FRN + TDM (CVPR-22) [23]	63.97	81.60	44.05	62.91
MCL (CVPR-22) [28]	64.66	81.31	44.08	64.61
MCL-Katz (CVPR-22) [28]	63.92	81.09	44.00	64.24
BiFRN (AAAI-23) [44]	66.07	83.30	46.64	66.46
Ours	**71.36**	**84.59**	**50.62**	**69.11**

robust generalization capabilities on novel classes. Experimental results also validate this claim.

3.5 Overall Objectives

After the SGNF module and GKPM module, we obtained the outputs of three layers: $(\tilde{\mathbf{f}}_l^Q, \mathbf{f}_l^P)$, $(\mathbf{f}_s^Q, \mathbf{f}_s^P)$, $(\mathbf{f}_t^Q, \mathbf{f}_t^P)$, we simplify the symbols to achieve a clearer representation, i.e. $(\mathbf{f}_m^Q, \mathbf{f}_m^P)$, where $m = \{l, s, t\}$, with $\tilde{\mathbf{f}}_l^Q$ simplified to $\mathbf{f}_l^Q$.

In a N-way K-shot training episodic, the loss function can be formulated as follows,

$$\mathcal{L}_m = -\frac{1}{N}\frac{1}{U}\sum_{i=1}^{N}\sum_{j=1}^{U} log \frac{\exp\left(\tau_m \mathcal{S}\left(\mathbf{f}_{i,j,m}^Q, \mathbf{f}_{i,m}^P\right)\right)}{\sum_{p=1}^{N}\exp\left(\tau_m \mathcal{S}\left(\mathbf{f}_{i,j,m}^Q, \mathbf{f}_{p,m}^P\right)\right)}, \qquad (18)$$

where τ_m are learnable scaling parameters and $\mathcal{S}(\cdot)$ represents the Cosine similarity to measure the similarity between query features and the prototype. The overall loss is calculated as

$$\mathcal{L} = \mathcal{L}_l + \mathcal{L}_s + \mathcal{L}_t. \qquad (19)$$

4 Experiments

4.1 Dataset

We use five widely-used few-shot fine-grained benchmark datasets, including **CUB-200-2011** [39], **Stanford Dogs** [19], **Stanford Cars** [20], **meta-iNat** [15, 42], and **tiered meta-iNat** [42]. We follow the commonly used standard dataset splitting way [43, 54], as shown in Tab. 1.

4.2 Implementation Details

For a fair comparison with previous work, we adopt two commonly used Conv-4 and ResNet-12 as the backbone networks, and both accepted input image sizes of 84 × 84.

Table 5: Ablation study of submodules using Conv-4 backbone on the CUB and Stanford-Dogs datasets.

Baseline	SGNF	GKPM	CUB		Stanford-Dogs	
			1-shot	5-shot	1-shot	5-shot
✓			68.03	81.92	55.85	71.35
✓	✓		75.08	87.03	60.64	75.98
✓		✓	72.68	85.32	60.29	74.82
✓	✓	✓	**79.19**	**89.71**	**67.33**	**81.08**

Meta-training Details: We employ common data augmentation techniques, such as random crop, horizontal flip, and color jitter, consistent with existing methods. For all benchmark datasets, we use SGD with Nesterov momentum of 0.9. The initial learning rate is set to 0.1 and weight decay to 5e-4. The α is set to 0.3.

Meta-testing Details: We apply the standard 5-way 1-shot and 5-way 5-shot settings. We save the best-performing model on the validation set to test. We report the 95% confidence interval results for 2,000 test episodes for all experiments.

4.3 Comparison with State-of-the-Art Methods

In this section, we compare our proposed method with a number of state-of-the-art methods, including general FSL methods (e.g. ProtoNet, DeepEMD, and FRN) and FS-FGIC methods (e.g. HelixFormer, AGPF, and BiFRN). The experimental results are shown in Table 2-4. Based on the experimental results, it can be observed:

Firstly, our proposed method outperforms state-of-the-art methods, achieving comprehensive performance leadership. This superiority is evident not only in typical fine-grained datasets (CUB, Stanford Cars, and Stanford Dogs) but also in more challenging fine-grained datasets (meta-iNat and tiered meta-iNat). Furthermore, compared to AGPF based on multi-scale feature aggregation, our method consistently exhibits performance improvements across all experimental settings. This not only indicates the importance of filtering out background and other trivial noise while introducing mid-level features, but also validates the effectiveness of the SGNF module. Additionally, under the 1-shot setting with only one support sample, our method demonstrates a more significant leading advantage, indirectly proving the effectiveness of BTG-Net in preventing overfitting. It also confirms that, by introducing the TG prompt, based on cross-task general knowledge learned, the model can be well generalized to novel tasks with very limited task-specific support samples. Finally, BTG-Net exhibits excellent performance on both Conv-4 and ResNet-12, showing nonsignificant overfitting with an increase in feature extractor parameters.

4.4 Analysis

To further demonstrate the effectiveness of the two modules and the rationality of the detailed designs within the modules, we conduct additional experiments and analyses.

4.4.1 Ablation study of submodules. In order to demonstrate the effectiveness of the two modules proposed, we conduct the module-wise ablation study as shown in Table 5. The experimental results demonstrate that both SGNK and GKPM enhance baseline performance. When the two modules are combined, the performance sees a significant further improvement, validating the effectiveness of the proposed method in addressing FS-FGIC tasks from both FGIC and FSL perspectives.

Table 6: Results of different layer integration ways in the SGNF module on the CUB and Stanford-Dogs datasets, where l, s, and t represent the outputs of the last layer, second-to-last layer, and third-to-last layer of the network respectively, Concat($\cdot$) refers to the concatenation operation, and SGNF(a, b) denotes that the SGNF preserves layers a and b.

Model	CUB		Stanford-Dogs	
	1-shot	5-shot	1-shot	5-shot
Baseline	68.03	81.92	55.85	71.35
Concat(l, s, t)	70.44	83.98	57.36	73.09
SGNF(l, s)	76.66	87.91	65.51	79.55
SGNF(l, t)	77.20	88.12	64.67	79.04
SGNF(l, s, t)	**79.19**	**89.71**	**67.33**	**81.08**

Table 7: Experimental results of removing the TG Prompt in the GKPM on the CUB and Stanford-Dogs datasets.

TG Prompt	CUB		Stanford-Dogs	
	1-shot	5-shot	1-shot	5-shot
w/o	78.02	89.07	65.56	79.86
w/	**79.19**	**89.71**	**67.33**	**81.08**

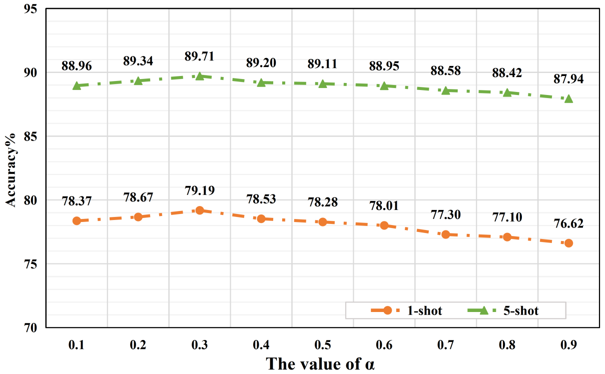

Figure 3: Classification performance of the BTG-Net with different values of α, using Conv-4 backbone on the CUB dataset.

4.4.2 Effectiveness analysis of SGNK. To demonstrate that the SGNK module is an ideal framework for leveraging the feature learning capability of the network in a multi-layer strategy, we conducted additional experiments, and the results are shown in Table 6. The results show that the concatenation operation of multiple layers inevitably introduces noise, leading to overfitting issues under the FSL setting, thus, the performance improvement is not significant.

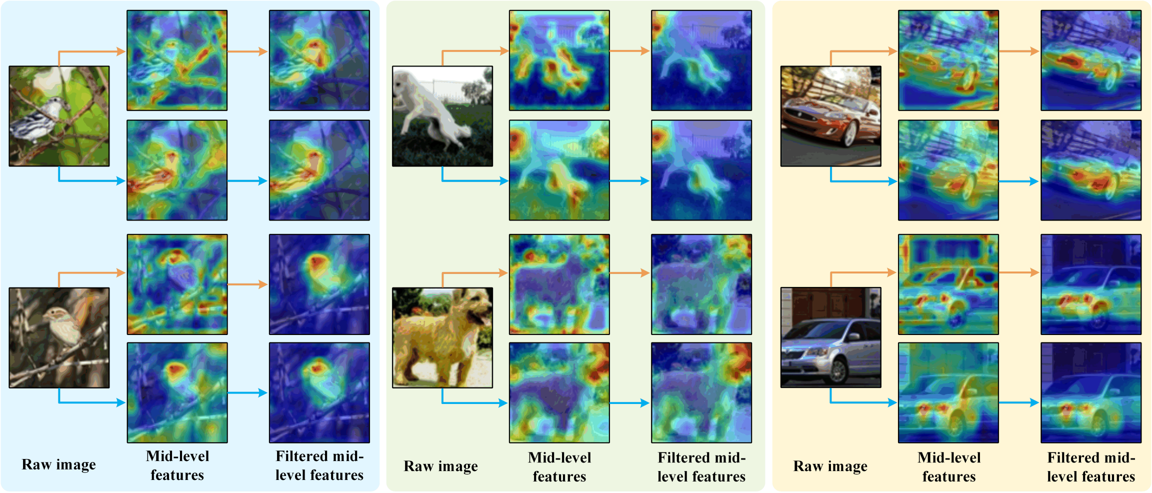
Raw image
Mid-level features
Filtered mid-level features
Raw image
Mid-level features
Filtered mid-level features
Raw image
Mid-level features
Filtered mid-level features

Figure 4: The visualization results of mid-level features and the filtered mid-level features corresponding to the raw image on the CUB, Stanford-Dogs and Stanford-Cars datasets.

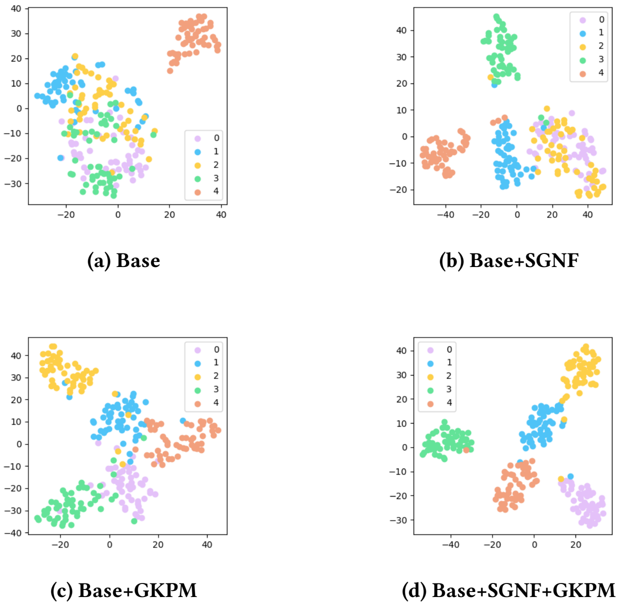

(a) Base

(b) Base+SGNF

(c) Base+GKPM

(d) Base+SGNF+GKPM

Figure 5: 5-way t-SNE visualization results of the embedding space on the CUB dataset, where different colors represent different classes. Randomly selecting five novel classes from the test set, and each class contains 50 query samples.

Therefore, it is essential to filter out background noise while introducing mid-level features, and the SGNK module designed in this paper proves to be the most effective structure.

4.4.3 Effectiveness analysis of TG Prompt in the GKPM. We conducted additional experiments with (w/) and without (w/o) TG Prompt, as shown in Table 7. The results indicate that TG Prompt contributes to performance improvement, further confirming that learning cross-task general knowledge is effective for FS-FGIC, and can enhance the generalization ability of the model on novel classes.

4.4.4 The influence of α. To better explore the impact of balancing hyperparameter α on model performance, we conducted additional experiments as shown in Figure 3. The experimental results indicate that setting the value of α to 0.3 leads to the highest classification accuracy. This indicates the necessity of hyperparameter α.

4.5 Visualization

To fully demonstrate the effectiveness of the SGNF module, we present additional visual results as shown in Figure 4. Based on the results, it can be observed that the proposed SGNF module effectively eliminates background noise in the mid-level features.

To better understand the effectiveness of each module from the perspective of feature mapping results, we also show the t-SNE visualization results in Figure 5. It can be observed that results generated by only a baseline model (Figure 5a) are unsatisfactory, with blurry class boundaries and many points of different classes intermingled. According to Figure 5d, it can be observed that, after combining SGNF and GKPM, each class forms a compact cluster and the boundaries between different clusters are obvious. This further demonstrates the effectiveness of SGNF and GKPM, then verifies that our proposed model has strong generalization ability and can learn optimized fine-grained features.

5 Conclusion

In this paper, we propose a novel Bi-directional Task-Guided Network (BTG-Net) for FS-FGIC. The BTG-Net consists of two modules. The Semantic-Guided Noise Filtering (SGNF) module effectively filters out noise such as background in mid-level features, and the General Knowledge Prompt Modeling (GKPM) module ensures robust generalization performance on novel classes by introducing cross-task general knowledge. Our proposed method achieves comprehensive leadership in performance on five benchmark datasets.

Acknowledgments

This work was supported in part by the National Natural Science Foundation of China under Grant 62202272, 62172256, 62202278, in part by Natural Science Foundation of Shandong Province under Grant ZR2019ZD06, ZR2020QF036, ZR2021ZD15, in part by the Young Scholars Program of Shandong University, and in part by the Major Program of the National Natural Science Foundation of China under Grant 61991411.

References

[1] Tom B. Brown, Benjamin Mann, Nick Ryder, and Melanie Subbiah et al. 2020. Language Models are Few-Shot Learners. In *NeurIPS*. 1877–1901.

[2] Chun-Fu (Richard) Chen, Quanfu Fan, and Rameswar Panda. 2021. CrossViT: Cross-Attention Multi-Scale Vision Transformer for Image Classification. In *ICCV*. 347–356.

[3] Zitian Chen, Yanwei Fu, Yinda Zhang, Yugang Jiang, Xiangyang Xue, and Leonid Sigal. 2019. Multi-Level Semantic Feature Augmentation for One-Shot Learning. *IEEE Transactions on Image Processing* 28, 9 (2019), 4594–4605.

[4] Hao Cheng, Siyuan Yang, Joey Tianyi Zhou, Lanqing Guo, and Bihan Wen. 2023. Frequency Guidance Matters in Few-Shot Learning. In *ICCV*. 11814–11824.

[5] Jun Cheng, Fusheng Hao, Liu Liu, and Dacheng Tao. 2022. Imposing Semantic Consistency of Local Descriptors for Few-Shot Learning. *IEEE Transactions on Image Processing* 31 (2022), 1587–1600.

[6] Carl Doersch, Ankush Gupta, and Andrew Zisserman. 2020. CrossTransformers: spatially-aware few-shot transfer. In *NeurIPS*. 21981–21993.

[7] Chuanqi Dong, Wenbin Li, Jing Huo, Zheng Gu, and Yang Gao. 2020. Learning Task-aware Local Representations for Few-shot Learning. In *IJCAI*. 716–722.

[8] Lintao Dong, Wei Zhai, and Zheng-Jun Zha. 2023. Exploring Tuning Characteristics of Ventral Stream's Neurons for Few-Shot Image Classification. In *AAAI*. 534–542.

[9] Alexey Dosovitskiy, Lucas Beyer, Alexander Kolesnikov, Dirk Weissenborn, Xiaohua Zhai, Thomas Unterthiner, Mostafa Dehghani, Matthias Minderer, Georg Heigold, Sylvain Gelly, Jakob Uszkoreit, and Neil Houlsby. 2021. An Image is Worth 16x16 Words: Transformers for Image Recognition at Scale. In *ICLR*.

[10] Fei Du, Peng Yang, Qi Jia, Fengtao Nan, Xiaoting Chen, and Yun Yang. 2023. Global and Local Mixture Consistency Cumulative Learning for Long-tailed Visual Recognitions. In *CVPR*. 15814–15823.

[11] Ruoyi Du, Dongliang Chang, Ayan Kumar Bhunia, Jiyang Xie, Zhanyu Ma, Yi-Zhe Song, and Jun Guo. 2020. Fine-Grained Visual Classification via Progressive Multi-granularity Training of Jigsaw Patches. In *ECCV*. 153–168.

[12] Chelsea Finn, Pieter Abbeel, and Sergey Levine. 2017. Model-Agnostic Meta-Learning for Fast Adaptation of Deep Networks. In *ICML*. 1126–1135.

[13] Bharath Hariharan and Ross B. Girshick. 2017. Low-Shot Visual Recognition by Shrinking and Hallucinating Features. In *ICCV*. 3037–3046.

[14] Kaiming He, Xiangyu Zhang, Shaoqing Ren, and Jian Sun. 2016. Deep Residual Learning for Image Recognition. In *CVPR*. 770–778.

[15] Grant Van Horn, Oisin Mac Aodha, Yang Song, Yin Cui, Chen Sun, Alexander Shepard, Hartwig Adam, Pietro Perona, and Serge J. Belongie. 2018. The INaturalist Species Classification and Detection Dataset. In *CVPR*. 8769–8778.

[16] Huaxi Huang, Junjie Zhang, Litao Yu, Jian Zhang, Qiang Wu, and Chang Xu. 2021. TOAN: Target-Oriented Alignment Network for Fine-Grained Image Categorization With Few Labeled Samples. *IEEE Transactions on Circuits and Systems for Video Technology* 32, 2 (2021), 853–866.

[17] Huaxi Huang, Junjie Zhang, Jian Zhang, Jingsong Xu, and Qiang Wu. 2021. Low-Rank Pairwise Alignment Bilinear Network For Few-Shot Fine-Grained Image Classification. *IEEE Transactions on Multimedia* 23 (2021), 1666–1680.

[18] Menglin Jia, Luming Tang, Bor-Chun Chen, Claire Cardie, Serge J. Belongie, Bharath Hariharan, and Ser-Nam Lim. 2022. Visual Prompt Tuning. In *ECCV*. 709–727.

[19] Aditya Khosla, Nityananda Jayadevaprakash, Bangpeng Yao, and Li Fei-Fei. 2011. Novel Dataset for Fine-Grained Image Categorization. In *CVPR Workshop*. 806–813.

[20] Jonathan Krause, Michael Stark, Jia Deng, and Li Fei-Fei. 2013. 3D Object Representations for Fine-Grained Categorization. In *ICCV Workshops*. 554–561.

[21] Jinxiang Lai, Siqian Yang, Junhong Zhou, Wenlong Wu, Xiaochen Chen, Jun Liu, Bin-Bin Gao, and Chengjie Wang. 2023. Clustered-patch Element Connection for Few-shot Learning. In *IJCAI*. 991–998.

[22] Kwonjoon Lee, Subhransu Maji, Avinash Ravichandran, and Stefano Soatto. 2019. Meta-Learning With Differentiable Convex Optimization. In *CVPR*. 10657–10665.

[23] Su Been Lee, WonJun Moon, and Jae-Pil Heo. 2022. Task Discrepancy Maximization for Fine-grained Few-Shot Classification. In *CVPR*. 5321–5330.

[24] Wenbin Li, Lei Wang, Jinglin Xu, Jing Huo, Yang Gao, and Jiebo Luo. 2019. Revisiting Local Descriptor Based Image-To-Class Measure for Few-Shot Learning. In *CVPR*. 7260–7268.

[25] Xiaoxu Li, Qi Song, Jijie Wu, Rui Zhu, Zhanyu Ma, and Jing-Hao Xue. 2023. Locally-Enriched Cross-Reconstruction for Few-Shot Fine-Grained Image Classification. *IEEE Transactions on Circuits and Systems for Video Technology* 33, 12 (2023), 7530–7540.

[26] Xiaoxu Li, Jijie Wu, Zhuo Sun, Zhanyu Ma, Jie Cao, and Jing-Hao Xue. 2021. BSNet: Bi-Similarity Network for Few-shot Fine-grained Image Classification. *IEEE Transactions on Image Processing* 30 (2021), 1318–1331.

[27] Bin Liu, Yue Cao, Yutong Lin, Qi Li, Zheng Zhang, Mingsheng Long, and Han Hu. 2020. Negative Margin Matters: Understanding Margin in Few-Shot Classification. In *ECCV*. 438–455.

[28] Yang Liu, Weifeng Zhang, Chao Xiang, Tu Zheng, Deng Cai, and Xiaofei He. 2022. Learning to Affiliate: Mutual Centralized Learning for Few-shot Classification. In *CVPR*. 14391–14400.

[29] Tsendsuren Munkhdalai, Xingdi Yuan, Soroush Mehri, and Adam Trischler. 2018. Rapid Adaptation with Conditionally Shifted Neurons. In *ICML*. 3661–3670.

[30] Andrei A. Rusu, Dushyant Rao, Jakub Sygnowski, Oriol Vinyals, Razvan Pascanu, Simon Osindero, and Raia Hadsell. 2019. Meta-Learning with Latent Embedding Optimization. In *ICLR*.

[31] Zhiqiang Shen, Zechun Liu, Jie Qin, Marios Savvides, and Kwang-Ting Cheng. 2021. Partial Is Better Than All: Revisiting Fine-tuning Strategy for Few-shot Learning. In *AAAI*. 9594–9602.

[32] Christian Simon, Piotr Koniusz, Richard Nock, and Mehrtash Harandi. 2020. Adaptive Subspaces for Few-Shot Learning. In *CVPR*. 4135–4144.

[33] Jake Snell, Kevin Swersky, and Richard S. Zemel. 2017. Prototypical Networks for Few-shot Learning. In *NeurIPS*. 4077–4087.

[34] Flood Sung, Yongxin Yang, Li Zhang, Tao Xiang, Philip H. S. Torr, and Timothy M. Hospedales. 2018. Learning to Compare: Relation Network for Few-Shot Learning. In *CVPR*. 1199–1208.

[35] Hao Tang, Zechao Li, Zhimao Peng, and Jinhui Tang. 2020. BlockMix: Meta Regularization and Self-Calibrated Inference for Metric-Based Meta-Learning. In *ACM MM*. 610–618.

[36] Hao Tang, Chengcheng Yuan, Zechao Li, and Jinhui Tang. 2022. Learning attention-guided pyramidal features for few-shot fine-grained recognition. *Pattern Recognition* 130 (2022), 108792.

[37] Luming Tang, Davis Wertheimer, and Bharath Hariharan. 2020. Revisiting Pose-Normalization for Fine-Grained Few-Shot Recognition. In *CVPR*. 14340–14349.

[38] Oriol Vinyals, Charles Blundell, Tim Lillicrap, Koray Kavukcuoglu, and Daan Wierstra. 2016. Matching Networks for One Shot Learning. In *NeurIPS*. 3630–3638.

[39] Catherine Wah, Steve Branson, Peter Welinder, Pietro Perona, and Serge Belongie. 2011. The Caltech-UCSD Birds-200-2011 Dataset. (2011).

[40] Chuanming Wang, Huiyuan Fu, and Huadong Ma. 2022. PaCL: Part-level Contrastive Learning for Fine-grained Few-shot Image Classification. In *ACM MM*. 6416–6424.

[41] Xiushen Wei, Peng Wang, Lingqiao Liu, Chunhua Shen, and Jianxin Wu. 2019. Piecewise Classifier Mappings: Learning Fine-Grained Learners for Novel Categories With Few Examples. *IEEE Transactions on Image Processing* 28, 12 (2019), 6116–6125.

[42] Davis Wertheimer and Bharath Hariharan. 2019. Few-Shot Learning With Localization in Realistic Settings. In *CVPR*. 6558–6567.

[43] Davis Wertheimer, Luming Tang, and Bharath Hariharan. 2021. Few-Shot Classification With Feature Map Reconstruction Networks. In *CVPR*. 8012–8021.

[44] Jijie Wu, Dongliang Chang, Aneeshan Sain, Xiaoxu Li, Zhanyu Ma, Jie Cao, Jun Guo, and Yi-Zhe Song. 2023. Bi-directional Feature Reconstruction Network for Fine-Grained Few-Shot Image Classification. In *AAAI*. 2821–2829.

[45] Yike Wu, Bo Zhang, Gang Yu, Weixi Zhang, Bin Wang, Tao Chen, and Jiayuan Fan. 2021. Object-aware Long-short-range Spatial Alignment for Few-Shot Fine-Grained Image Classification. In *ACM MM*. 107–115.

[46] Shulin Xu, Faen Zhang, Xiushen Wei, and Jianhua Wang. 2022. Dual Attention Networks for Few-Shot Fine-Grained Recognition. In *AAAI*. 2911–2919.

[47] Yun Yang, Yuanyuan Hu, Xingyi Zhang, and Song Wang. 2022. Two-Stage Selective Ensemble of CNN via Deep Tree Training for Medical Image Classification. *IEEE Transactions on Cybernetics* 52, 9 (2022), 9194–9207.

[48] Han-Jia Ye, Hexiang Hu, De-Chuan Zhan, and Fei Sha. 2020. Few-Shot Learning via Embedding Adaptation With Set-to-Set Functions. In *CVPR*. 8805–8814.

[49] Zican Zha, Hao Tang, Yunlian Sun, and Jinhui Tang. 2023. Boosting Few-Shot Fine-Grained Recognition With Background Suppression and Foreground Alignment. *IEEE Transactions on Circuits and Systems for Video Technology* 33, 8 (2023), 3947–3961.

[50] Bo Zhang, Jiakang Yuan, Baopu Li, Tao Chen, Jiayuan Fan, and Botian Shi. 2022. Learning Cross-Image Object Semantic Relation in Transformer for Few-Shot Fine-Grained Image Classification. In *ACM MM*. 2135–2144.

[51] Chi Zhang, Yujun Cai, Guosheng Lin, and Chunhua Shen. 2020. DeepEMD: Few-Shot Image Classification With Differentiable Earth Mover's Distance and Structured Classifiers. In *CVPR*. 12200–12210.

[52] Kaiyang Zhou, Jingkang Yang, Chen Change Loy, and Ziwei Liu. 2022. Conditional Prompt Learning for Vision-Language Models. In *CVPR*. 16795–16804.

[53] Kaiyang Zhou, Jingkang Yang, Chen Change Loy, and Ziwei Liu. 2022. Learning to Prompt for Vision-Language Models. *International Journal of Computer Vision* 130, 9 (2022), 2337–2348.

[54] Yaohui Zhu, Chenlong Liu, and Shuqiang Jiang. 2020. Multi-attention Meta Learning for Few-shot Fine-grained Image Recognition. In *IJCAI*. 1090–1096.